RSC Applied Interfaces

ROYAL SOCIETY OF CHEMISTRY

PAPER

View Article Online
View Journal | View Issue

Cite this: *RSC Appl. Interfaces*, 2025, **2**, 451

Solid-lubrication properties of copper benzene-1,4-dicaboxylate, a metal–organic framework with a two-dimensional layered crystal structure†

Hiroshi Eguchi, *[a] Sara Kato,[a] Satoru Maegawa,[b] Fumihiro Itoigawa[b] and Kenji Nagata[a]

Solid lubricants are widely used to control friction and wear in moving contact areas. In particular, inorganic materials with layered crystal structures, such as graphite, are a well-known category of solid lubricant. However, their structural designability is restricted because of their chemically stable nature, making it difficult to control their tribological characteristics. In this study, the solid lubricity of copper(II) benzene-1,4-dicarboxylate (CuBDC), a two-dimensional metal–organic framework (2D-MOF), was investigated as a new type of solid lubricant with structural diversity. The tribological measurements of powder-supported specimens revealed that CuBDC exhibited good lubrication properties comparable to those of typical solid lubricants, such as graphite and polytetrafluoroethylene. From the scanning electron microscopy observations of the worn surfaces of the CuBDC-supported specimen, the layered crystal structure of CuBDC effectively formed a smooth wear surface at the contact area. In contrast, specimens supporting copper(II) benzoate and copper(II) benzene-1,3,5-tricarboxylate, which have similar chemical natures as CuBDC, exhibited high frictional force, reflecting on the difference in their crystal structures. Furthermore, the transformation of the CuBDC crystal by thermal treatment, which afforded interlayer coordination bonds, increased the friction coefficient. These results suggest that the solid lubricity of CuBDC originates from its layered crystal structure. Thus, the 2D-MOFs with layered crystal structures are potential candidates for solid lubricants with good property tunability.

Received 25th July 2024,
Accepted 2nd December 2024

DOI: 10.1039/d4lf00267a

rsc.li/RSCApplInter

Introduction

For sustainable development, it is highly important to reduce the friction and wear of sliding surfaces. According to literature, 23% of all energy in human society is consumed to overcome frictional forces and reproduce worn mechanical parts.[1] To reduce friction, various types of lubricants, such as oil, grease, and solid lubricants, are used in both the industry and everyday life. Among them, solid lubricants can be used under specific conditions where lubricants with fluidity are not suitable, *i.e.*, ultra-low temperatures, high vacuum conditions, and environments in which contaminations must be avoided.[2–4] As representative solid lubricants, soft metals, fluorine-containing polymers, and some inorganic particles with two-dimensional (2D)-layered crystal structures are widely used.[5–9]

Graphite and transition metal dichalcogenide—specifically molybdenum and tungsten disulfide—with 2D-layered crystal structures are known as solid lubricants.[10,11] Their weakly interacted layers can easily be cleaved by shear force under sliding surfaces to exhibit solid lubricity. They have been utilized widely because of their lubricity, chemical and thermal stability, and availability. Another example of layered solid lubricants is clays, *e.g.*, mica and montmorillonite, whose intercalated alkaline metal cation is exchangeable to others, such as alkylammonium cations.[12–14] This intercalation modification of clay facilitates the control of the interactions between layers, tuning their solid lubricities depending on the structures of cation species. More recently, some transition metal carbide/nitride, called MXenes, have attracted considerable attention as a new solid lubricant owing to their high mechanical properties and modifiability for surface characteristics.[15,16] However, the designability of the layered crystal structures and tunability of their properties are still limited for the conventional solid lubricants mentioned above. Therefore, developing novel materials with structural diversity is important to achieve the

[a] *Department of Life Science and Applied Chemistry, Graduate School of Engineering, Nagoya Institute of Technology, Gokiso-cho, Showa-ku, Nagoya 466-8555, Japan. E-mail: eguchi.hiroshi@nitech.ac.jp*
[b] *Department of Electrical and Mechanical Engineering, Nagoya Institute of Technology, Gokiso-cho, Showa-ku, Nagoya 466-8555, Japan*

† Electronic supplementary information (ESI) available. See DOI: https://doi.org/10.1039/d4lf00267a

fabrication of tailor-made solid lubricants for the recent requirements in various application fields such as robotics, space engineering, and microelectromechanical systems (MEMS).

As candidates for solid lubricants, metal–organic frameworks (MOFs) are attractive materials owing to their distinctive features. The structure of MOFs consists of transition metal ions and organic linkers, forming coordination bonds to fabricate polymeric crystalline materials.[17] They have been deployed for various applications in gas separation,[18] energy storage,[19] molecular recognition,[20,21] and polymer composite.[22] MOFs have substantial structural designability because of the variation of organic linkers and the combinations with metal ions. Using planar coordination units to prepare MOFs, 2D-MOFs with layered crystal structures can be fabricated. Compared with conventional solid lubricants, the lubricities of 2D-MOFs are tunable by designing the structures. Therefore, 2D-MOFs can be employed as solid lubricants that complement conventional ones (Fig. 1a). Furthermore, Liu and coworkers have recently revealed that the highly smooth surfaces of 2D-MOF crystals exhibit solid superlubricity under nanotribological experimental conditions using atomic force microscopy techniques.[23,24] These results strongly encourage the application of 2D-MOFs as solid lubricants in macroscopic uses.

In this study, we demonstrate the solid lubricity of copper benzene-1,4-dicarboxylate (CuBDC), a known 2D-MOF with a layered crystal structure (Fig. 1b). Copper(II) cation and carboxylate anion form a paddle-wheel-type $Cu_2(COO)_4$ secondary building unit (SBU); thus, the linear ligand of benzene-1,4-dicarboxylate provides a square planar MOF structure.[25] The tribological characteristics of CuBDC as a solid lubricant are evaluated with ball-on-disk friction tests, and the worn surface is observed by scanning electron microscopy (SEM). The relationship between the lubrication properties and crystal structure is revealed by comparing the series of the related coordination compounds with different numbers of carboxylate moieties, indicating that the layered crystal structure is essential for solid lubricity. Additionally, the effect of the crystal transformation of CuBDC by thermal treatment on its solid lubricity is discussed.

Experimental

Materials

A filter paper (Φ30 mm × 0.26 mm, cellulose, minimum retention particle size is 5 μm) was obtained from Advantec (Tokyo, Japan). Copper(II) acetate monohydrate, benzene-1,4-dicarboxylic acid, and benzene-1,3,5-tricarboxylic acid were purchased from the Tokyo Chemical Industry (Tokyo, Japan). Dimethylformamide (DMF) was supplied from Fujifilm Wako Pure Chemical (Osaka, Japan). Ethanol and *tert*-butanol were obtained from Nacalai Tesque (Kyoto, Japan). Polytetrafluoroethylene (PTFE, 10 μm) and graphite platelets (25 μm) were purchased from Sigma-Aldrich (Steinheim, Germany). Silica powder (colloidal silica, 19–84 nm for primary particles and ~15 μm for secondary particles) was supplied from Kanto Chemical (Tokyo, Japan). All chemicals were used as received.

Characterization

SEM observations were performed on a JSM-IT200 instrument (JEOL, Tokyo, Japan). All sample surfaces were coated with a thin Pt layer using a JEC-3000FC Auto Fine Coater (JEOL, Tokyo, Japan) before SEM observation. Powder X-ray diffraction (PXRD) analyses were carried out on SmartLab SE (Rigaku, Osaka, Japan) equipped with a Cu Kα X-ray source and a D/tex Ultra250 1D detector. Fourier transfer infrared (FT-IR) spectroscopy measurements were carried out on FT/IR-6700 (JASCO, Tokyo, Japan) using an attenuated total reflection method. X-ray photoelectron spectroscopy (XPS) characterizations were performed on a PHI Quantes system

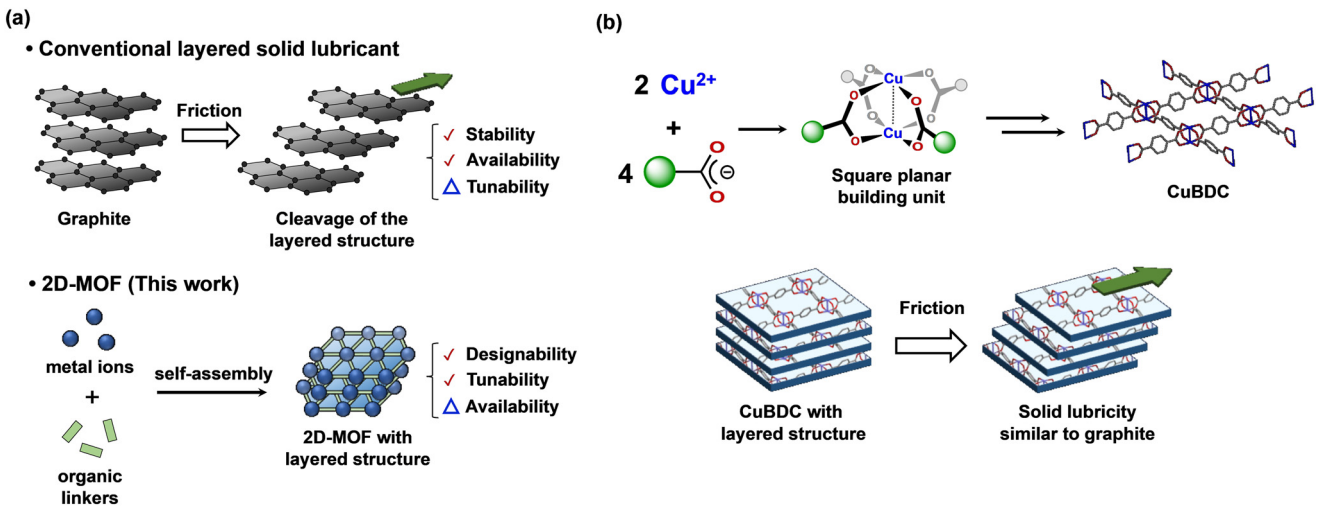

Fig. 1 Solid lubricants with a layered structure: (a) schematic of the lubrication mechanism of graphite and the structural feature of the two-dimensional metal–organic frameworks (2D-MOFs); (b) preparation of square-planar $Cu_2(COO)_4$ building unit and copper(II) benzene-1,4-carboxylate (CuBDC) and the concept of its solid lubrication properties.

(ULVAC-PHI, Kanagawa, Japan) with an Al K_α X-ray source and a detection angle of 45°. Tribological experiments were performed on a lab-made reciprocating ball-on-disk tribometer. A 6-axis force-torque sensor (PFS-55YA251U6, Leptrino, Nagano, Japan) with ±0.125 N force resolution and an auto liner moving stage (KXL06030, Suruga Seiki, Shizuoka, Japan) were used as a friction sensor and mechanical sliding device, respectively. The friction coefficient data were plotted as a moving average for clarity.

Synthetic procedures of the coordination compounds

Copper benzene-1,4-dicarboxylate. According to a reported procedure,[25] CuBDC was prepared as follows: copper(II) acetate monohydrate (0.800 g, 4.00 mmol) was added to a round bottom flask containing a solution of benzene-1,4-dicarboxylic acid (0.667 g, 4.00 mmol) in DMF (90 mL). After mixing the suspension for several minutes, the reaction flask was placed in an oil bath at 110 °C without stirring. After 36 h at that temperature, the reaction mixture was cooled to ambient conditions, and the resulting dispersed solid was collected by vacuum filtration using a membrane filter. The obtained blue solid was sequentially washed with DMF, methanol, and acetone. Thereafter, the solid was dispersed in *tert*-butanol by sonication and subsequently freeze-dried to obtain CuBDC as a blue powder (yields: 1.07 g).

Copper benzene-1,3,5-tricarboxylate. The preparation procedure of copper benzene-1,3,5-tricarboxylate (CuBTC) was the same as that of CuBDC, except that the ligand was replaced with benzene-1,3,5-tricarboxylic acid, and 1.33 equivalents relative to copper(II) acetate were used (yields: 0.59 g).

Copper benzoate. According to a reported procedure,[26] copper benzoate (CuBMC) was prepared as follows: copper(II) acetate monohydrate (0.995 g, 5.00 mmol) was added to a round bottom flask containing a solution of sodium benzoate (1.41 g, 10.0 mmol) in tetrahydrofuran (80 mL). The reaction mixture was refluxed for 12 h, and after cooling to ambient temperature, the suspension was filtered. The volatile organics in the filtrate were removed under reduced pressure. The resulting solid was dispersed in *tert*-butanol by sonication and subsequently freeze-dried to obtain CuBMC as a blue powder (yields: 0.83 g).

Tribological experiments

A specimen for friction test was prepared as follows: solid lubricant powder was dispersed in ethanol by sonication and deposited onto a cellulose filter paper by vacuum filtration. Thereafter, it was dried at 100 °C and fixed onto cardboard using an epoxy adhesive. The obtained specimens were attached to the sliding stage of the reciprocating tribometer. A steel ball (Φ4.8 mm, SUJ-2) was used as a counterpart, and a normal load of 5.0 N was applied. Since a cellulose filter paper was compressed by a counterpart to proceed with plastic deformation in this experimental condition, the actual normal load was considered rather than the Hertzian contact pressure. A sliding distance was set up to 10 mm, with a maximum sliding speed of 10 mm s^{-1} at the half point. The frictional force was recorded at a sampling rate of 10 Hz, reaching 1000 reciprocating cycles (approximately 2400 s). To clarify the friction coefficient *vs.* time curves, the moving average value for 10 s was plotted on the graphs. All specimens were evaluated at least three times to check their reproducibility.

Results and discussion

Using a solvothermal method, CuBDC was synthesized as a blue powder (Fig. 2a). To obtain fine particles of CuBDC for measuring the solid lubricity, CuBDC was dispersed in *tert*-butanol by sonication; thereafter, a freeze-drying process was carried out. The powdery CuBDC was redispersed in ethanol and supported onto a filter paper by vacuum filtration to obtain a specimen for friction test (Fig. 2b). The PXRD pattern of the obtained powder was good in accordance with the simulation based on the single-crystal structure reported previously (Fig. 2c),[25] indicating that the layered structure incorporated the DMF molecules coordinated to an apical position of copper atoms. From the observation of the surface of the CuBDC-supported specimen, there were many cracks in a filter cake whose width was 20–50 μm (Fig. 2d), presumably because of the drying process. Additionally, a maximum particle size of 2 μm was observed, and the particles aggregated to form the filter cake. Further, graphite-, PTFE-, and silica-supported specimens were prepared using the same procedure. Similar surface morphologies with cracks were observed in the silica-supported specimen, and the surfaces of the graphite- and PTFE-supported specimens were relatively uniform (Fig. S1 in ESI†).

The solid lubricities of CuBDC and other powders were evaluated with ball-on-disk reciprocating friction tests (Fig. 3a and b, Φ4.8 mm SUJ-2 steel ball was used as a counterpart, and a normal load of 5 N was applied). Fig. 3c shows the friction coefficient changes during the measurements of various specimens. For a filter paper without supported particles, the friction coefficient rapidly increased during the first 200 s, and finally, it reached a steady state, in which the friction coefficient was 0.63. The friction coefficient was increased because of the contact-area expansion with the compression of the filter paper fibers at the sliding surface. Similarly, a silica-supported specimen exhibited almost the same friction coefficient of 0.64, indicating that silica particles did not play a role as a solid lubricant. In contrast, the CuBDC-supported specimen exhibited considerably different characteristics. That is, the friction coefficient slightly decreased to ~0.20 for the first 200 s and maintained that value during the measurement period (2400 s). This result was reproducible even when the preparation condition of CuBDC was changed (Fig. S12 in ESI†). To clarify the solid lubricity of CuBDC, friction tests of specimens supporting other solid lubricants were conducted. Resultantly, the friction coefficients of the graphite- and PTFE-supported specimens under steady state were

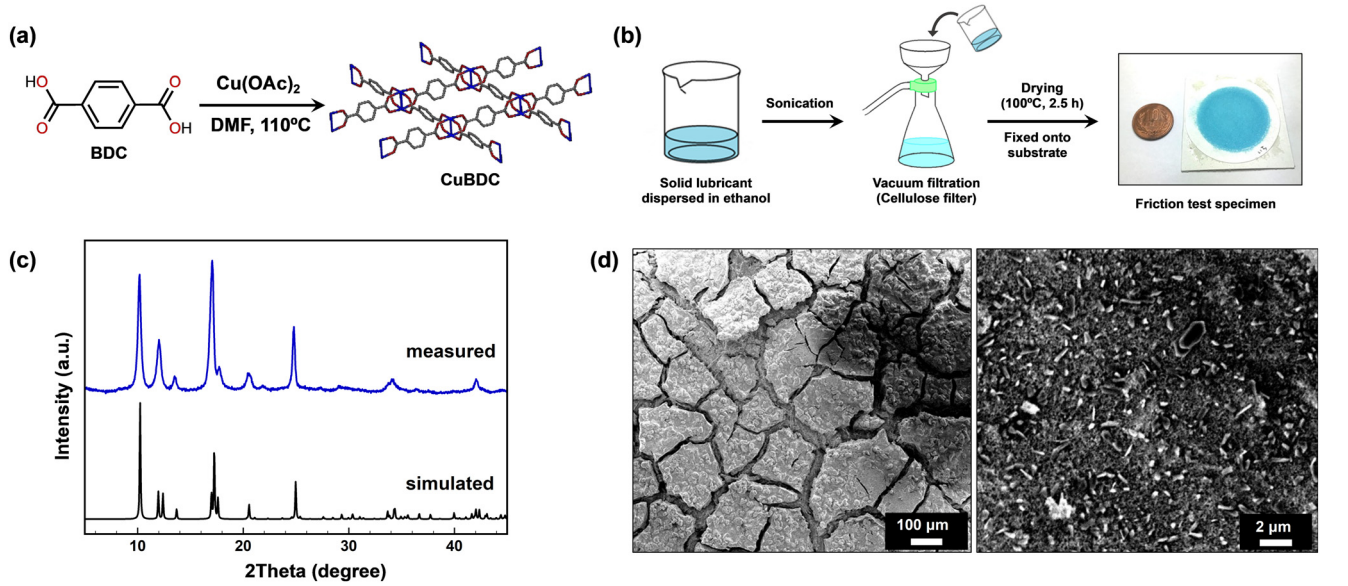

Fig. 2 Preparation of the CuBDC-supported specimen: (a) synthesis of CuBDC using a solvothermal method; (b) preparation procedure of the specimens supporting the powder; (c) measured and simulated powder X-ray diffraction patterns of CuBDC, in which the latter one was calculated based on the single-crystal structure reported in ref. 25; (d) scanning electron microscopy (SEM) images of the surface of the CuBDC-supported specimen.

determined to be 0.28 and 0.14, respectively. In the case of the graphite-supported specimen, the friction coefficient slightly increased in the early stage of the friction test (~100 s), which would originate from the relatively thick filtration cake of graphite (Fig. S4 in ESI†). The graphite particles were roughly packed in the cake at the initial state and gradually compressed by a counterpart during the friction test along with the expansion of the contact area. Thus, until the tightly compressed surface was formed, the friction coefficient was slightly increased. From the above, the solid lubricity of

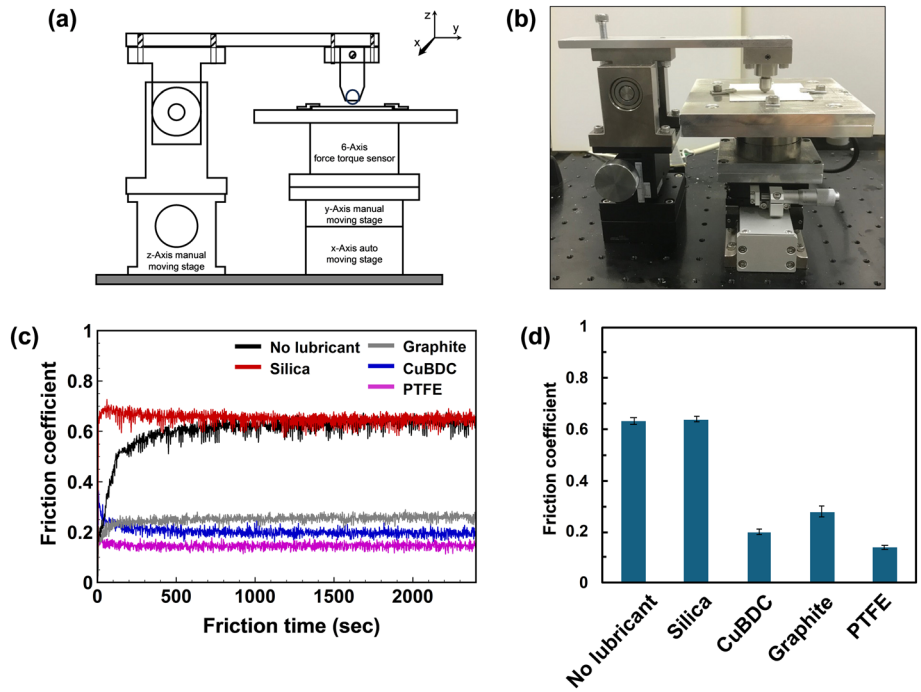

Fig. 3 Characterization of the solid tribological properties on the powder-supported specimens: (a and b) schematic and optical images of the reciprocating tribometer; (c) friction coefficient *vs.* time curves of the specimens against a steel-ball counterpart; (d) friction coefficient of the specimens at the steady state (error bar: standard deviation).

CuBDC was almost comparable to that of representative solid lubricants (Fig. 3d), presumably because of the layered crystal structure.

To investigate the role of the supported solid particles, the surfaces of the specimens after the friction test were observed using SEM (Fig. 4). On the worn surface of the pristine filter paper, cellulose fibers were compressed, forming a highly rough morphology with fractures of fibers. In contrast, the worn surface of the silica-supported specimen was relatively smooth, presumably because the colloidal silica particles filled the spaces between the compressed fibers. For the CuBDC-supported specimen, the worn surface was relatively smooth, exhibiting a morphology like the structure of hair cuticles. That indicates that a lubrication layer consisting of CuBDC formed on the surface of the sliding area. Further, a similar morphology was observed on the worn surface of the graphite-supported specimen, indicating that they had similar lubrication mechanisms. The worn surface of the PTFE-supported specimen displayed a slightly different morphology, where the shapes of cellulose fiber were still distinguishable. To obtain further insight, the cross-sections of the worn specimens were observed using SEM-EDS (Fig. S5–S7 in ESI†). PTFE particles were located not only on the worn surface but also in the space between the cellulose fibers, where some fibers remain to be exposed to the surface of specimens. In contrast, CuBDC and graphite formed continuous lubrication layers on the top of the worn surface. These differences would mainly originate from the characteristics of the particles. That is, particles with lamellar platelet shapes like CuBDC and graphite strongly tend to spread laterally by shear force. Therefore, CuBDC would act similarly to graphite under the experimental conditions, resulting in a low friction coefficient (~0.20).

In general, the lubricities of solid lubricants originate from the reducing interfacial shear stresses between contact surfaces. To clarify the role of CuBDC under the sliding surface, its interfacial shear stresses in the tribotests were discussed. The frictional force is represented by the following equation:

$$F = A_r \times s,$$

where F is a frictional force, A_r is a real contact area, and s is the interfacial shear stress.[27] To all the specimens, the widths of the wear tracks ranged from 1.1 to 1.3 mm, indicating that their apparent contact areas were comparable. Further, judging from the surface morphologies observed by SEM, there were no critical differences in the roughness of the contact areas, except for that of the pristine filter paper, indicating that the real contact areas between the counterpart and the specimens were similar. Therefore, the differences between the frictional forces were mainly dependent on the difference in the shear stress. For the silica-supported specimen, a high friction coefficient (0.64) was measured despite the relatively smooth surface similar to that of other specimens, which was due to the high interfacial shear stress

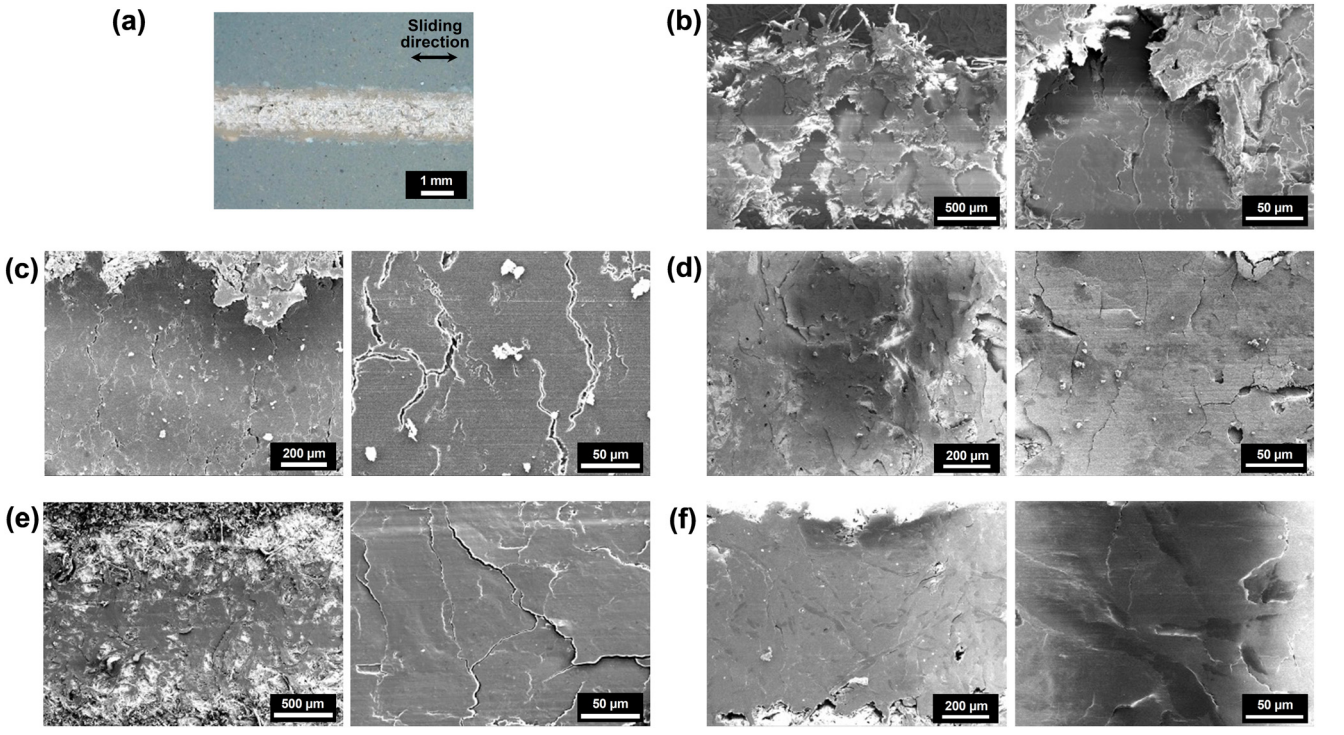

Fig. 4 Microscopic observations of the worn surfaces: (a) representative optical microscope image of the worn surface (CuBDC-supported specimen); SEM images of the worn surfaces of (b) pristine filter paper and the (c) silica-, (d) CuBDC-, (e) graphite-, and (f) polytetrafluoroethylene-supported specimens.

between silica and a steel counterpart. In contrast, owing to the low shear stresses derived from the weekly interacted lamellar structure, the specimens supporting graphite exhibited a low friction coefficient (0.28). For CuBDC, a similar lubrication mechanism, namely the cleavages of the layered structure with weak interaction,[28] was assumed.

To elucidate the transfer film formation, the composition of the surface of the steel ball after the friction test was evaluated. After blowing the steel surface to remove the attached powders, XPS measurements were performed with Φ100 μm X-ray beam which was sufficiently smaller than the width of the contact area (~400 μm, Fig. S8a in ESI†). Based on the survey scan analysis (Fig. S8b in ESI†), it was revealed that 64 atom% of C and 32 atom% of O were absorbed on the steel surface after the friction test. In addition, approximately 1 atom% of copper was also detected. To investigate the details, a high-resolution spectrum of C 1s was also measured (Fig. S8c in ESI†). In the spectrum, the two peaks attributable to aromatic sp^2 C–C and COO group were observed at 284.5 eV and 289.0 eV, respectively, suggesting that the surface of the counterpart was covered with the ligand of CuBDC. Furthermore, the latter peak was shifted from that of the pristine CuBDC (288.2 eV), presumably due to the hydrolysis of copper carboxylate (COOCu) structure to form dicarboxylic acid during the friction test.[29] Therefore, the transfer film fabricated by the friction of CuBDC mainly consisted of the ligand rather than the pristine 2D-MOF structure.

Next, the effect of the layered crystal structure of CuBDC on the solid lubricity was examined. The three-dimensional crystal structure of MOFs depends on the geometries of both SBUs and organic linkers, and the connectivity of the SBUs can be modified by changing the chemical structures of the ligand molecules. For CuBDC, if the ligand was replaced with benzoic acid or benzene-1,3,5-tricarboxylic acid, coordination compounds with zero-dimensional and three-dimensional structures (CuBMC and CuBTC, respectively) can be fabricated (Fig. 5a).[26,30] This series of coordination compounds with similar chemical composition but different SBU connectivity was regarded as a good model to investigate the effects of crystal structure on the solid lubricity of MOFs. Therefore, the tribological characteristics of CuBMC and CuBTC were evaluated. Both CuBMC and CuBTC were prepared according to the reported literature, and the obtained powders were retained onto filter paper as mentioned above. The SEM observations of the surfaces revealed that the particle of CuBTC exhibited a chunk shape with a size from 5 to 20 μm (Fig. 5b). In contrast, the morphology of CuBMC was porous, and individual particles were undistinguishable by the SEM image, indicating that the primary particle size would be less than sub micrometers. Regarding both specimens, there were cracks in the filter cakes similar to the case of CuBDC.

The friction coefficient curves of the CuBMC- and CuBTC-supported specimens are shown in Fig. 5c with the result of CuBDC. It shows that their solid lubricities are significantly affected by their crystal structures. In all cases, the friction state changed to a steady state within the first 200 s, where the order

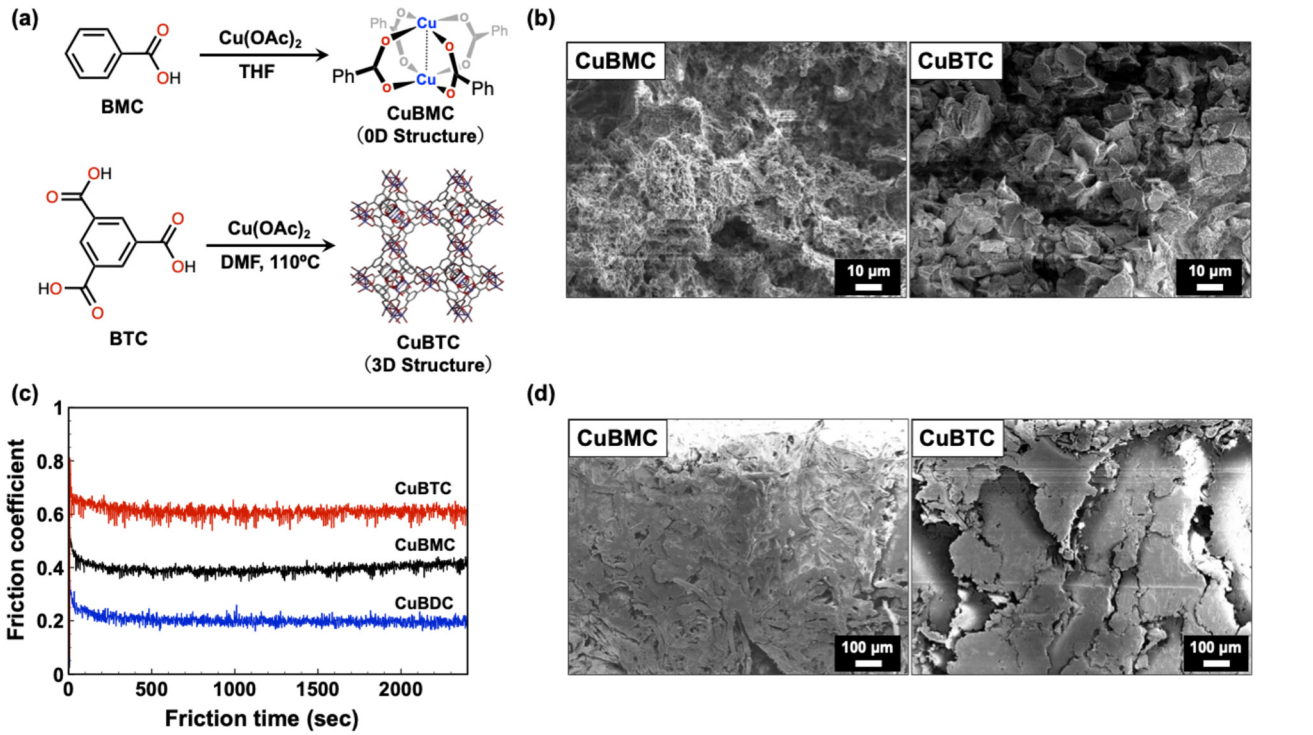

Fig. 5 Evaluation of the coordination compounds with related structures to CuBDC: (a) synthesis of copper benzoate (CuBMC) and copper benzene-1,3,5-tricarboxylate (CuBTC); (b) SEM images of the CuBMC- and CuBTC-supported specimens; (c) friction coefficient *vs.* time curves of the specimens against a steel-ball counterpart; (d) SEM images of the worn surfaces of the specimens.

of their friction coefficient was CuBTC (0.62) > CuBMC (0.38) > CuBDC (0.20). Regarding the result of CuBTC, the three-dimensionally connected crystal structure did not cleave easily by shear stress. Furthermore, the particles of CuBTC were relatively large (up to approximately 20 μm), which would cause their exclusion from the contact surface by sliding a ball. Therefore, direct contact between the ball and cellulose fiber occurred and caused severe damage on the worn surface, similar to the case of the specimen without solid particles (Fig. 5d). In contrast, there were no destructive fractures of fibers on the worn surface of the CuBMC-supported specimen. Owing to the potentially fragile nature of the CuBMC crystal, which did not have coordination bonds between SBUs, the formation of the tiny particles was induced by frictional force to fill the space between the cellulose fibers. Resultantly, the surface roughness was controlled to a moderate level, and the direct contact between the cellulose fibers and a counterpart was partially suppressed, maintaining a low friction coefficient. However, the fibrous morphology was still observable on the surface, and effective lubrication layers were not fabricated compared with the case of CuBDC. These results suggested that the solid lubrication property of CuBDC originated from its 2D crystal structure.

Furthermore, the effect of the transformation of the crystal structure was investigated. Recently, Jing *et al.* reported that CuBDC underwent a change in crystal structure upon heating at 250 °C under vacuum conditions, in which incorporated DMF molecules coordinated to the apical position of the paddle-wheel SBU were evaporated.[31] Thereafter, new coordination bonds were formed between a copper atom with a vacant site and an oxygen atom of the carboxylate group located in an adjacent layered structure (Fig. 6a). Consequently, the thermal treatment of CuBDC provided a three-dimensionally connected crystal structure, indicating the increase in the friction coefficient because of the loss of the cleavable interfaces. The thermal treatment of powdery CuBDC was carried out as reported in the literature to obtain a transformed compound (CuBDC-heat). Thermal gravimetric analysis revealed that the temperature at the start of the weight loss increased from ~200 °C to ~300 °C, indicating the removal of the coordinated solvent (Fig. 6b). Further, this was supported by the FT-IR spectra, where the peak originated from dimethylformamide observed at 1664 cm^{-1} disappeared after thermal treatment (Fig. S11 in ESI†). Additionally, a peak attributable to the antisymmetric COO^- stretching mode was shifted from 1608 cm^{-1} to 1586 cm^{-1} reflecting on their coordination environments,[25,31] although an unidentified minor peak also appeared at 1550 cm^{-1} which was presumably due to the irregular hydrolysis. Furthermore, the PXRD pattern before and after thermal treatment completely changed, indicating that the transition of the crystal structure successfully proceeded (Fig. S10 in ESI†). Subsequently, the solid lubricity of CuBDC-heat was evaluated as described earlier. Resultantly, the friction coefficient of the CuBDC-heat-supported specimen was recorded to be 0.68 (Fig. 6c), which was considerably higher than that of pristine CuBDC (0.20). The SEM observation of the worn surface indicated a rough morphology similar to that of the CuBTC-supported specimen, indicating that a lubricating film did not form on the substrate because of the loss of the layered crystal structure.

Conclusions

In conclusion, we demonstrated the solid lubrication properties of CuBDC, a 2D-MOF, and its lubrication mechanism was discussed. CuBDC exhibited a good performance comparable to

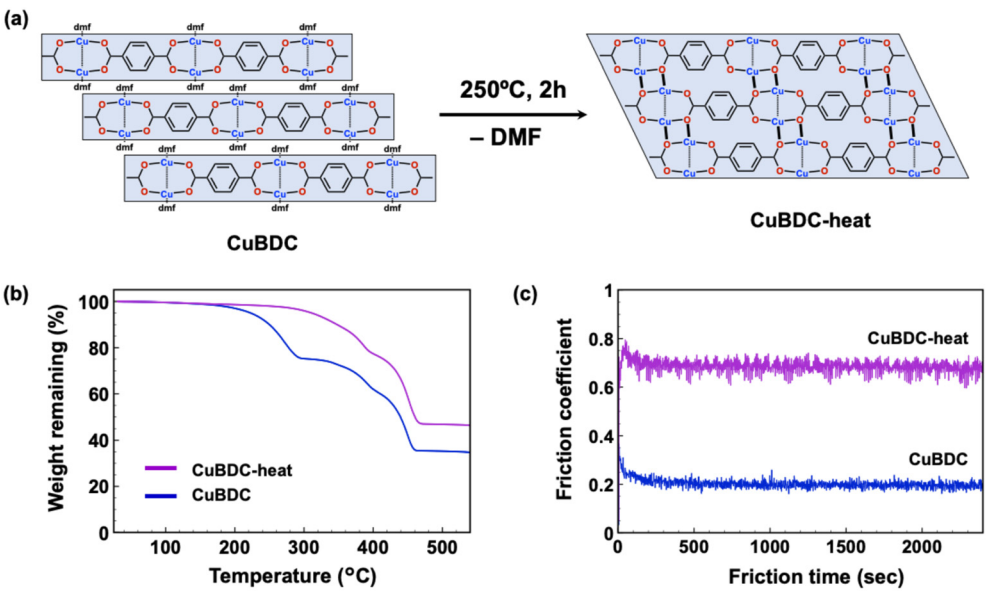

Fig. 6 Transformation of the crystal structure of CuBDC: (a) schematic image of the structural change in the crystal structure of CuBDC by thermal treatment; (b) thermal gravimetric analyses of CuBDC before and after thermal treatment; (c) friction coefficient *vs.* time curve of the CuBDC- and CuBDC-heat-supported specimens.

that of representative solid lubricants, graphite and PTFE, and the SEM observation revealed that CuBDC formed a smooth surface on a substrate during the friction test. To elucidate the lubrication mechanism of CuBDC, comparative experiments with the structurally related copper-containing coordination compounds were carried out. Furthermore, the effect of the crystal transformation of CuBDC into the non-layered structure was investigated. These results indicated that the layered structure of CuBDC would be an essential factor for exhibiting its solid lubricities. An advantage of 2D-MOF-based solid lubricants is the designability of their structural and chemical features, which provides the opportunity to tune the tribological performance. Our current research focuses on expanding this concept to other coordination compounds and their practical applications.

Data availability

The data supporting this article have been included as part of the ESI.†

Author contributions

H. E. designed the main conceptual ideas and wrote the original draft of the manuscript. H. E. and S. K. planned the experiments and analyzed the data. S. K. performed the experiments and collected the data. S. M. and F. I. provided important insight into the tribological characterization. K. N. supervised the study. All authors discussed the results and commented on the manuscript.

Conflicts of interest

There are no conflicts to declare.

Acknowledgements

This work was supported by JSPS KAKENHI Grant-in-Aid for Early-Career Scientists (23K13558), the Tatematsu Foundation, and the Suzuki Foundation. The XPS measurements were carried out at the Equipment Sharing Division, Organization for Co-Creation Research and Social Contributions, Nagoya Institute of Technology. The authors thank Mr. Yukihisa Moriguchi and Ms. Yoko Yamazaki for performing XPS measurements.

References

1 K. Holmberg and A. Erdemir, Influence of tribology on global energy consumption, costs and emissions, *Friction*, 2017, **5**, 263–284.
2 T. W. Scharf and S. V. Prasad, Solid lubricants: a review, *J. Mater. Sci.*, 2013, **48**, 511–531.
3 H. Hedayati, A. Mofidi, A. Al-Fadhli and M. Aramesh, Solid Lubricants Used in Extreme Conditions Experienced in Machining: A Comprehensive Review of Recent Developments and Applications, *Lubricants*, 2024, **12**, 69.
4 J. R. Lince, Effective Application of Solid Lubricants in Spacecraft Mechanisms, *Lubricants*, 2020, **8**, 74.
5 N. Xiao, C. Zhang, X. Yin, K. Yang, F. Zhang and B. Xiong, Soft metal micro/nanolubricant in tribology, *Mater. Sci. Eng., B*, 2023, **295**, 116600.
6 J. Ye, D. Burris and T. Xie, A Review of Transfer Films and Their Role in Ultra-Low-Wear Sliding of Polymers, *Lubricants*, 2016, **4**, 4.
7 Y. Guo, X. Zhou, K. Lee, H. C. Yoon, Q. Xu and D. Wang, Recent development in friction of 2D materials: from mechanisms to applications, *Nanotechnology*, 2021, **32**, 312002.
8 D. Berman, A. Erdemir and A. V. Sumant, Approaches for Achieving Superlubricity in Two-Dimensional Materials, *ACS Nano*, 2018, **12**, 2122–2137.
9 X. Zhang, T. Ren and Z. Li, Recent advances of two-dimensional lubricating materials: from tunable tribological properties to applications, *J. Mater. Chem. A*, 2023, **11**, 9239–9269.
10 W. Huai, C. Zhang and S. Wen, Graphite-based solid lubricant for high-temperature lubrication, *Friction*, 2021, **9**, 1660–1672.
11 T. Polcar and A. Cavaleiro, Self-adaptive low friction coatings based on transition metal dichalcogenides, *Thin Solid Films*, 2011, **519**, 4037–4044.
12 K. Oshita, M. Yanagi, Y. Okada and S. Komiyama, Tribological properties of a synthetic mica-organic intercalation compound used as a solid lubricant, *Surf. Coat. Technol.*, 2017, **325**, 738–745.
13 K. Oshita, S. Komiyama and S. Sasaki, Intercalation Technology for Preparing a Mica–Organic Hybrid Solid Lubricant and Spectroscopic Evaluation of Its Lubrication Mechanism, *Tribol. Online*, 2019, **14**, 312–320.
14 K. Oshita, S. Komiyama and S. Sasaki, FTIR observation of cleavage state of a mica–organic hybrid solid lubricant under reciprocating sliding conditions, *Tribol. Int.*, 2019, **130**, 74–84.
15 B. C. Wyatt, A. Rosenkranz and B. Anasori, 2D MXenes: Tunable Mechanical and Tribological Properties, *Adv. Mater.*, 2021, **33**, 2007973.
16 P. Serles, M. Hamidinejad, P. G. Demingos, L. Ma, N. Barri, H. Taylor, C. V. Singh, C. B. Park and T. Filleter, Friction of $Ti_3C_2T_x$ MXenes, *Nano Lett.*, 2022, **22**, 3356–3363.
17 V. F. Yusuf, N. I. Malek and S. K. Kailasa, Review on Metal–Organic Framework Classification, Synthetic Approaches, and Influencing Factors: Applications in Energy, Drug Delivery, and Wastewater Treatment, *ACS Omega*, 2022, **7**, 44507–44531.
18 S. Yu, C. Li, S. Zhao, M. Chai, J. Hou and R. Lin, Recent advances in the interfacial engineering of MOF-based mixed matrix membranes for gas separation, *Nanoscale*, 2024, **16**, 7716–7733.
19 J. Ren, Y. Huang, H. Zhu, B. Zhang, H. Zhu, S. Shen, G. Tan, F. Wu, H. He, S. Lan, X. Xia and Q. Liu, Recent progress on MOF-derived carbon materials for energy storage, *Carbon Energy*, 2020, **2**, 176–202.

20 B. Chen, S. Xiang and G. Qian, Metal–Organic Frameworks with Functional Pores for Recognition of Small Molecules, *Acc. Chem. Res.*, 2010, **43**, 1115–1124.
21 N. Hosono and T. Uemura, Metal-Organic Frameworks for Macromolecular Recognition and Separation, *Matter*, 2020, **3**, 652–663.
22 M. Kalaj, K. C. Bentz, S. Ayala, J. M. Palomba, K. S. Barcus, Y. Katayama and S. M. Cohen, MOF-Polymer Hybrid Materials: From Simple Composites to Tailored Architectures, *Chem. Rev.*, 2020, **120**, 8267–8302.
23 L. Liu, Y. Zhang, Y. Qiao, S. Tan, S. Feng, J. Ma, Y. Liu and J. Luo, 2D metal-organic frameworks with square grid structure: A promising new-generation superlubricating material, *Nano Today*, 2021, **40**, 101262.
24 L. Liu, K. Wang, Y. Liu and J. Luo, The relationship between surface structure and super-lubrication performance based on 2D MOFs, *Appl. Mater. Today*, 2022, **26**, 101382.
25 C. G. Carson, K. Hardcastle, J. Schwartz, X. Liu, C. Hoffmann, R. A. Gerhardt and R. Tannenbaum, Synthesis and Structure Characterization of Copper Terephthalate Metal–Organic Frameworks, *Eur. J. Inorg. Chem.*, 2009, **16**, 2338–2343.
26 J. A. Solera-Rojas, L. Krause, M. L. Montero, D. Stalke and L. W. Pineda, Synthesis and Crystal Structure of a Copper(II) Benzoate Complex Bearing a Bis-2,2′-Tetrahydrofuryl Peroxide Moiety, *J. Chem. Crystallogr.*, 2018, **48**, 138–144.
27 X. He, Z. Liu, L. B. Ripley, V. L. Swensen, I. J. Griffin-Wiesner, B. R. Gulner, G. R. McAndrews, R. J. Wieser, B. P. Borovsky, Q. J. Wang and S. H. Kim, Empirical relationship between interfacial shear stress and contact pressure in micro- and macro-scale friction, *Tribol. Int.*, 2021, **155**, 106780.
28 Z. Zeng, I. S. Flyagina and J.-C. Tan, Nanomechanical behavior and interfacial deformation beyond the elastic limit in 2D metal–organic framework nanosheets, *Nanoscale Adv.*, 2020, **2**, 5181–5191.
29 M. Rosillo-Lopez and C. G. Salzmann, *RSC Adv.*, 2018, **8**, 11043.
30 S. S.-Y. Chui, S. M.-F. Lo, J. P. H. Charmant, A. G. Orpen and I. D. Williams, A Chemically Functionalizable Nanoporous Material $[Cu_3(TMA)_2(H_2O)_3]_n$, *Science*, 1999, **283**, 1148–1150.
31 Y. Jing, Y. Yoshida, P. Huang and H. Kitagawa, Reversible One- to Two- to Three-Dimensional Transformation in Cu^{II} Coordination Polymer, *Angew. Chem., Int. Ed.*, 2022, **61**, e202117417.